

## SPECIAL ISSUE PAPER

**Detail-feature-preserving surface reconstruction**Xu Zhao<sup>1</sup>, Zhong Zhou<sup>1\*</sup>, Ye Duan<sup>2</sup> and Wei Wu<sup>1</sup><sup>1</sup> State Key Laboratory of Virtual Reality Technology and Systems, School of Computer Science and Engineering, Beihang University, Beijing, China<sup>2</sup> Computer Graphics and Image Understanding Lab, Department of Computer Science, University of Missouri – Columbia, Columbia, MO, USA**ABSTRACT**

In this paper, we propose a feature-preserving surface reconstruction method from sparse noisy 3D measurements such as range scanning or passive multiview stereo. In contrast to earlier methods, we define a novel type of explicit 3D filter—regularized weighted least squares filter—to characterize the detail features such as surface wrinkles and sharp features. To account for noise, we rasterize input-oriented points into a probabilistic volume (base volume) and then create a guidance volume by Gaussian filtering. Both the base volume and the guidance volume are further filtered by regularized weighted least squares filter to detect and recover detail features. After the two-stage filtering, a global minimal surface is computed by graph cut and meshed as a geometric model. Experimental results on various datasets show that our method is robust to noise, outliers, and missing parts, which makes it more suitable to fit indoor/outdoor multiview stereo data. Unlike other methods, our method can completely recover scene structures and preserve detail features from noisy point samples. Copyright © 2012 John Wiley & Sons, Ltd.

**KEYWORDS**

surface reconstruction; computational geometry; computer graphics

**\*Correspondence**

Zhong Zhou, State Key Laboratory of Virtual Reality Technology and Systems, School of Computer Science and Engineering, Beihang University, Beijing, China.

E-mail: zz@vrlab.buaa.edu.cn

**1. INTRODUCTION**

Reconstructing 3D surfaces from point samples is well studied in many areas of computer graphics, including laser scanning, reconstructing image-based surfaces, and repairing of noisy meshes [1]. It focuses on approximately fitting a surface to point samples, filling holes, or remeshing existing models with the use of information about the sampling process, for example, bounds on the noise magnitude or the sampling density.

There are many approaches for acquiring 3D shapes from real-world objects, which can be basically classified into two categories: active lighting systems and passive stereo systems. Active lighting systems, such as laser-based scanners, structured light scanners, and infrared light devices, can produce more stable and accurate point samples than passive stereo systems. Recently, however, the passive stereo systems have become increasingly popular for their low-cost acquiring devices and attractive indoor/outdoor applications [2,3]. Unfortunately, most surface reconstruction algorithms cannot be directly used for passive stereo systems. For example, in passive multiview stereo, reconstructed point samples are seriously

affected by insufficient images, illumination changes, calibration errors, poor photo-consistent matches, and the structure and appearance of the scene to be reconstructed. Until recently, it has been a challenge to perform surface fitting from such poor point samples.

The latest surface reconstruction algorithms, such as Poisson surface [4] and touch expand [5], alleviate the poor data fitting problem to some extent and are widely used in image-based modeling systems. The key objective of these two methods is to define a surface-fit quality function from oriented points and then solve this optimization function. It is important to note that they all implicitly use a Gaussian filter in their algorithms to avoid the influence of noise and outliers and to achieve a smooth mesh model. They perform well in many cases especially when the surface of the reconstructed object is inherently smooth. But the smooth shape prior assumption also ignores some important detail features such as surface wrinkles as well as sharp edges and corners that occur widely in natural and artificial objects. Meanwhile, when considering points obtained using multiview stereo, detail features are difficult to distinguish from the noisy or incomplete point samples because both details and noise are high-frequency signals.

To solve these problems, we present a novel feature-preserving filter called regularized weighted least squares (RWLS) filter. The key idea is to define the detail features as the covariances between the input and a Gaussian-smoothed intermediate result. Also, a regularization parameter is added into the kernel function to balance the two. To account for noise, we first rasterize oriented points into a probabilistic volume (also called base volume) and create a guidance volume by Gaussian filtering. This filtering is completed using a large filter radius to ensure the reconstruction completeness and suppress noise as well as details. Only the significant high-frequency features that are defined as detail features are detected and recovered during RWLS filtering. Finally, meshes are generated from the filtered volume by graph cut.

The advantages of our method include the following: (1) the method has the ability to recover both sharp features as well as surface wrinkle features, and the level of detail can be easily controlled by adjusting filter parameters; and (2) the method is robust to noise, outliers, and missing parts, which cannot only be used for range scan data fitting but is also suitable for indoor/outdoor multiview data.

## 2. RELATED WORK

The earliest surface reconstruction methods are primarily designed for fitting 3D laser scanner data. They can be roughly classified into two major categories: implicit surface methods and Delaunay-based methods.

The goal of implicit surface methods is to implicitly define a level-set surface function such as signed distance function [6], radial basis function [7], or moving least squares (MLS) [8]. Among them, the MLS scheme can approximate the local surface from the point set with a moderate amount of noise, and various methods are further developed to improve its stability [9] or preserve sharp features [10]. However, they always fail when the points are irregularly sampled (e.g., incomplete) or too noisy. The idea behind MLS is to perform a local polynomial fitting in weighted least squares (WLS) sense, which can also be seen as an optimization-based filter kernel. Similarly, we define an RWLS filter for surface reconstruction. However, there are two differences in our method: (1) the filtering process is computed in 3D probabilistic space; (2) a guidance volume is generated by Gaussian filtering to suppress more noise and ensure the reconstruction completeness. Note that the 2D RWLS filter has been recently proposed in an image processing area [11]. Its applications include haze removal, image matting, high dynamic range (HDR) compression, noise reduction, and others [12]. An extensive literature search led to the conclusion that our method is the first attempt to extend the filter to 3D digital geometry processing, which led to its successful application in detail-feature-preserving surface reconstruction.

Delaunay-based methods typically interpolate all or most of the points on the basis of combinatorial structures, such as Delaunay triangulations [13], alpha shapes [14],

or Voronoi diagrams [15]. More recent work focuses on combining with other techniques such as partitioning strategy [16], variation method [17], or energy optimization framework [18] to improve the robustness to noise, outliers, and irregular sampling. Most notably, Salman *et al.* [19] addressed the problem of generating surface meshes from 3D point samples while preserving sharp features. They explicitly extract sharp features on the basis of the covariance matrices of Voronoi cells and then perform a feature-preserving variant of a Delaunay refinement process. However, most of these methods are not designed for the passive stereo system.

For the problem of surface reconstruction from multi-view stereo (MVS) point sets to be solved, shape priors and probabilistic optimization framework are often used. The basic shape prior assumes that the surface to be reconstructed is smooth, which yields to a regularized optimization problem [5,20]. Poisson surface [4] and touch expand [5] are two typical surface reconstruction algorithms and are widely applied in MVS reconstruction for their robustness. Kazhdan *et al.* [4] aligned the gradient of the indicator function with a vector field from the input-oriented points and compute it as a Poisson problem. Lempitsky and Boykov's global optimization approach [5] is based on the minimal surface framework with graph cuts in [21] and expresses the generic surface-to-data fit quality measurement as a flux-based function. Both methods implicitly use the Gaussian filter to handle sample noise, which is equivalent to the smoothness shape priors. Nevertheless, in practice, we found that if the filter radius is large, both implicit model and globalization methods will obtain a complete but oversmooth model. However, if the filter radius is small, a detailed but incorrect geometric model is produced. In many cases, both the completeness (scene structure) and surface details are crucial to the perception of 3D models. However, it is hard to make a trade off between them. Unlike these methods, our method first creates a guidance volume by Gaussian filtering and then recovers detail features by RWLS filtering. The two-stage filtering ensures that the resulting model can contain both complete structures and detail features. Moreover, the RWLS filter parameters can be easily adjusted to control the level of detail features to be preserved. Recently, more shape priors such as planar plane [22] and basic geometric shape primitives [23] are introduced. However, these assumptions are more suitable for urban scenes, whereas the local shape priors in RWLS filter are adaptively determined within a given neighborhood and have no limitation of scene types.

## 3. METHOD OVERVIEW

The overall goal of our method is to reconstruct a mesh surface from well/poor-sampled oriented points, to ensure the completeness and to recover detail features as much as possible. Figure 1 illustrates the basic step-by-step process of our surface reconstruction method, which consists

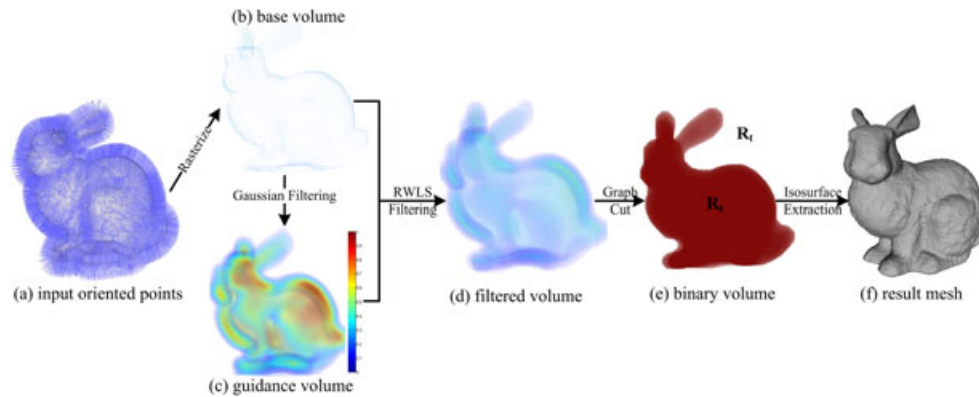


**Figure 1.** The overview of our surface reconstruction method. Oriented points (a) are first rasterized into a probabilistic base volume (b). A complete but oversmoothing guidance volume (c) is created by Gaussian filtering with a large radius. Regularized weighted least squares (RWLS) filter is then applied to the base and guidance volumes to preserve detail features (d). Desired surface corresponds to  $s/t$ -cut on the constructed graph (e) and is finally extracted as mesh model (f).

of four main phases: point sample rasterization, two-stage filtering, surface segmentation via graph cut, and isosurface extraction.

In the first rasterization phase, we fuse oriented points (Figure 1(a)) into a base volume (Figure 1(b)). The base volume is a probabilistic volume in which each voxel is assigned a divergence value representing the probability of a point belonging to the true surface. This phase also helps us to solve the surface reconstruction problem in MRF optimization framework.

The base volume has the most details but may also contain noise, holes, and outliers. The first step of the following two-step filtering phase is to apply a Gaussian filter with a large radius. The result is a guidance volume that is overly smoothed, but complete and without noise, as shown in Figure 1(c). Then, we define the detail features as the covariances between the base volume and the guidance volume and implicitly detect and recover them by RWLS filtering, as illustrated in Figure 1(d). The two-stage filtering not only preserves surface details but also ensures reconstruction completeness.

In the last two phases, we segment the filtered volume into interior and exterior via the graph cut algorithm [21]. Adjacent nodes are connected via  $n$ -links representing area-based regularization cost, whereas  $t$ -links connect nodes to the terminals  $R_s$  or  $R_t$  according to each voxel's filtered divergence value, as shown in Figure 1(e). A surface  $S$  corresponds to an  $s/t$ -cut on the constructed graph. Finally, we extract an isosurface from the binary segmented volume to get the final mesh model [24] (Figure 1(f)). In the following sections, we will focus on the first two phases in detail.

#### 4. POINT SAMPLE RASTERIZATION

Considering that the input point samples may contain noise, outliers, and missing parts, we rasterize the input-oriented points into a regular grid (also called base

volume). Each cell of the grid (also called a voxel) contains zero or several point samples (also called vectors  $\{x_p\}$ ). We assume that a voxel is closer to the true surface when more points are in the voxel. This can be quantified as the flux for the vector field. According to the Gauss–Ostrogradsky (also known as divergence) theorem, the flux is equivalent to the vector field's divergence  $\text{div}(x_p)$ , which can be computed by adding the gradient values of all vectors in each voxel. As a result, every voxel in the base volume is assigned a divergence value representing the probability of a voxel belonging to the true surface. After being normalized, these values can be seen as the intensities of image pixels, except that positive and negative values indicate whether the voxel is inside or outside of the surface.

Note that this phase also helps us solve the surface reconstruction problem within the MRF optimization framework, which can be expressed as the following minimization problem:

$$\arg \min_S \left( \int_S \lambda ds - \int_{\text{inter}(S)} \text{div}(x_p) dp \right), \quad (1)$$

where  $\{x_p\}$  is the vector field representing point samples. The parameter  $\lambda$  is an area-based regularization term, which can be chosen as a constant or according to the sampling density. Instead of directly solving Equation (1) by graph cut, we first apply two filters to ensure the reconstruction completeness and preserve detail features. We will discuss this in the next section.

#### 5. TWO-STAGE FILTERING

After rasterizing points into the base volume, we perform a two-stage filtering. In the first stage, a Gaussian filter with a large radius is applied to remove noise and outliers as well as fill holes. In the second stage, we apply a novel RWLS

filter to detect and recover detail features. Both filters can be expressed as a general 3D filtering process:

$$q_i = \sum_j W_{ij}(v_i; s_0, s_1, \dots) p_j, \quad (2)$$

where  $p$  and  $q$  respectively denote the base volume and the output filtered volume and  $i$  and  $j$  are voxel indexes, which indicate the corresponding divergence values. The kernel function  $W$  is the local filter operator with several parameters  $s = [s_0, s_1, \dots]$ .  $v$  is the guidance volume, which can be ignored in some filter operators, for example, Gaussian filter.

### 5.1. Gaussian Filtering

In the first stage, we apply a Gaussian filter to make the reconstructed surface smoother. We choose a large radius for the Gaussian filter in order to fill holes and ensure the reconstruction completeness. The result volume may be oversmoothed, but it keeps the basic shape of surface topology. It will be reserved as the guidance volume for the next stage filtering.

The Gaussian filter behaves similarly with the weighted average filter in the discrete approximation case. When the standard deviation  $\sigma$  is a constant, the kernel function only depends on the filter radius  $r$ . The weight parameters  $s = [s_0, s_1, \dots]$  can be pre-computed by the following:

$$s_n = \frac{e^{-n^2/2\sigma^2}}{\sum_{m \in r} e^{-m^2/2\sigma^2}} \quad (3)$$

We extend the integral image technique [25] to 3D volume and implement the 3D box filter that can approximately replace the Gaussian filter. Both the input base volume and the Gaussian-smoothed volume are used for the next stage filtering to recover detail features.

### 5.2. Detail-Feature-Preserving Filtering

Unlike other surface reconstruction methods that explicitly extract features and refine the surface, we implicitly detect and recover detail features in the RWLS filtering stage. The detail features include surface wrinkles and sharp edges or corners, which can be expressed as the differences between base volume and guidance volume. In RWLS kernel function, we quantify them as the covariances between the base volume and the guidance volume. Detail features will be restored from the base volume if and only if these values are significant.

Specifically, we define a novel filter, named RWLS filter, to preserve detail features. Similar to the traditional MLS surface [8], the WLS filter kernel parameters can adaptively be determined by local shape fitting in least squares sense:

$$\arg \min_s \sum_j (g_s - p_i)^2 \phi(\|p_i - p_j\|), \quad (4)$$

where  $g_s$  corresponds to the local approximation polynomial of the surface and  $\phi(p)$  denotes the spatial weight function. In general, the higher the degree of the polynomial, the more accurate the surface fitting result will be [9]. However, when the voxels are assigned with probabilities instead of point positions, the linear kernel function is good enough to fit. Therefore, we assume that the output volume  $q$  is a linear transform of  $v$  in a 3D window  $w_k$  centered at the voxel  $k$ :

$$q_i = g_s = a_k v_i + b_k, \forall i \in w_k, \quad (5)$$

where  $(a_k, b_k)$  are linear coefficients assumed to be constant in  $w_k$ . If we take a differential operator to both sides of Equation (5), we have  $\nabla q = a \nabla v$ . This means that the linear filter kernel ensures that the output volume has the same basic structure as the guidance volume. Meanwhile, coefficient  $a$  has an important effect on these structures. Moreover, we add a regularization term to the WLS kernel function in the window  $w_k$ :

$$\arg \min_{(a_k, b_k)} \sum_{i \in w_k} \left( (a_k v_i + b_k - p_i)^2 + \varepsilon a_k^2 \right), \quad (6)$$

where  $\varepsilon$  is a regularization parameter controlling the level of surface details. We solve this minimization problem by linear regression. Then, the RWLS filter kernel parameters can be explicitly determined by the following:

$$a_k = \frac{\text{cov}_k(v, p)}{\text{var}_k(v) + \varepsilon} = \frac{\frac{1}{|w|} \sum_{i \in w_k} v_i p_i - \frac{\mu_k}{|w|} \sum_{i \in w_k} p_i}{\sigma_k^2 + \varepsilon}. \quad (7)$$

$$b_k = \bar{p}_k - a_k \mu_k = \frac{1}{|w|} \sum_{i \in w_k} p_i - a_k \mu_k. \quad (8)$$

Here,  $\mu_k$  and  $\sigma^2$  are the mean and variance of  $v$  in 3D window  $w_k$ , whereas  $|w|$  is the number of voxels in  $w_k$ .

The definition of RWLS filter Equations (7) and (8) can also be implemented via box filter, because the equation form is basically  $\sum_{i \in w_k} f_i$ . We will further investigate the behavior of RWLS filter parameters in the next section.

### 5.3. Regularized Weighted Least Squares Filter Analysis

Intuitively, we take 2D line fitting to illustrate the behavior of the RWLS filter as shown in Figure 2. Here, we assume that the guidance layer is always a straight line. For simplicity, divergence values on the surface are set to one and the others equal zero.

When the base layer is also a straight line or has no signals (Figure 2(a)), the filtered output remains the same to the guidance layer because  $\text{cov}(v, p) = 0 \Rightarrow q_i = b_i = p_i$ . Another case is that the base layer is curve and

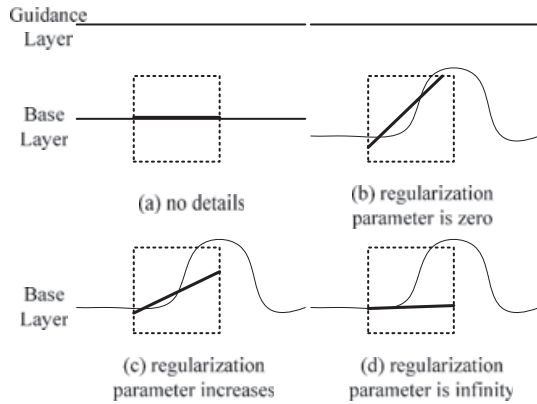


**Figure 2.** Two-dimensional line fitting example of regularized weighted least squares filter. The regularization parameter controls the detail levels.

different from guidance layer (Figure 2(b)–(d)). If the regularization parameter is zero, the filter kernel is simplified to a linear WLS filter function and the output becomes  $q_i = \frac{1}{|w_i|} \sum_{i \in w_k} (a_k v_i + b_k)$ . As shown in Figure 2(b), detail features are preserved by local filtering. If the regularization parameter increases,  $a_k$  becomes smaller and the filtered output is closer to the guidance layer as shown in Figure 2(c). If the regularization parameter tends to infinity,  $a_k$  tends to zero and the filtered output becomes the same as the guidance layer again (Figure 2(d)).

In other words, the detail levels can be controlled by the parameter  $\varepsilon$  in RWLS filtering. The surface patches with variance much larger than  $\varepsilon$  ( $\sigma^2 \gg \varepsilon$ ) are preserved detail features. Detail features belonging to surface patches with variance much smaller than  $\varepsilon$  ( $\sigma^2 \ll \varepsilon$ ) are closed to the guidance volume. Meanwhile, the radius of the 3D window determines the scale of detail features to be recovered. Small-scale detail features cannot be well reconstructed when the radius is too large.

On the basis of the property of RWLS filter, we assert that the two-stage filtering can preserve detail features while ensuring that the surface reconstruction process is robust to noise, outliers, and missing parts. Take 2D shape fitting as an example, shown in Figure 3. First, the Gaussian filtering with a large radius in the first stage ensures that the guidance volume is robust to noise (Figure 3(a)) and holes (Figure 3(b)). Meanwhile, the surface may be over-smoothed as shown in Figure 3(c). However, because the surface patches around sharp features have a large covariance value between guidance volume and base volume, the RWLS filtering will further detect these features and recover them from the base volume. Note that the covariance may also be large at noisy patches, but the fitting result is nearly the same to the guidance volume because noise is always randomly distributed. Patches around holes are similar to the guidance volume because the covariance is zero. Finally, the locality of the filtering ensures that the outliers do not affect the reconstructed result, as shown in Figure 3(d).

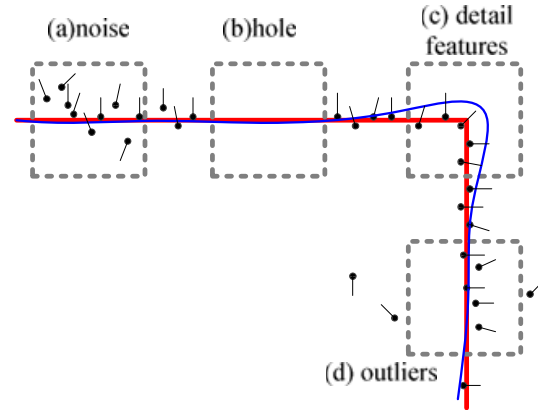


**Figure 3.** Two-dimensional example analysis of surface reconstruction with two-stage filtering. Guidance volume (blue line) is first created by Gaussian filter to ensure that the fitting shape is robust to noise, outliers, and missing parts. Next, regularized weighted least squares filter implicitly detects and recovers sharp features (red line) because of the large covariance between the base volume and the guidance volume.

As mentioned previously, the parameters of RWLS filter have an important effect on surface reconstruction. For the challenging MVS point sets, we present a method to determine the filter parameters according to the MVS reconstruction process. Assume that the largest image resolution is  $m$ , the cell size is  $n$  (at least one point will be reconstructed in  $n \times n$  pixel square region), and the photoconsistency matching windows size is  $s$ . We respectively set the Gaussian filter radius and the RWLS filter radius to  $\frac{2s}{n}$  and  $\frac{s}{n}$ . The latter one also implies the uncertainty of MVS reconstruction. The volume resolution can be assigned in  $[\frac{m}{s}, \frac{m}{n}]$ . Generally, the larger the volume resolution chosen, the better the visualization result achieved. The choice of regularization parameter  $\varepsilon$  depends on the variation of guidance volume. After multiplying normalized divergence values by a scale factor ( $\gamma = 2000$ ), we statistically calculate a mean variation value of about 1000. So, we set  $\varepsilon$  to 100, and it works well for most datasets.

## 6. EXPERIMENTAL RESULTS

In this section, we test our surface reconstruction method on various datasets including range scan data from Stanford (Figure 1), computer-aided design (CAD) data, and multiview stereo data from Middlebury [2] and Furukawa [26]. We also compare our method with Poisson surface [4] and touch expand [5]. By default, we set the octree depth to eight in Poisson surface for all the datasets, and the volume resolution and filter radius in touch expand algorithm are equal to the parameters of RWLS filter. The reason why we do not compare with other kernel-based methods (e.g., [10]) is that most of them are not designed to preserve features from noisy or incomplete point samples such as multiview stereo data. All datasets and

**Table I.** Summary of parameters used for each dataset in experiments.

Scene	Point no.	Image no.	Image size	Grid size	RWLS filter parameters
Bunny	34,835	–	–	$201 \times 200 \times 161$	$r = 3, \varepsilon = 100$
CAD	50,000	–	–	$202 \times 202 \times 137$	$r = 6, \varepsilon = 100$
Temple	17,370	312	$640 \times 480$	$102 \times 154 \times 77$	$r = 3, \varepsilon = 100$
Hall	213,682	61	$3008 \times 2000$	$201 \times 316 \times 316$	$r = 3, \varepsilon = 100$

RWLS, regularized weighted least squares.

their parameters are listed in Table I. For the MVS data, the point samples are computed by patch-based multi-view stereo (PMVS) algorithm [26] (cell size  $n = 2$  and photoconsistency matching windows size  $s = 7$ ), and most parameters are determined using the method described in Section 5.3.

We experiment the running time in a PC with 3.0 Hz Intel Core 2 Duo CPU (Intel Corporation, Santa Clara, CA, USA). The first two phases cost less than 60 s for all datasets listed in Table I. However, most of the time (several minutes or more) is consumed during the other two phases, especially when performing the graph cut with a large volume resolution.

### 6.1. Fitting to Simulated CAD Data

In this experiment, we show that our method is robust in four different cases. Case 1: The input point cloud is well sampled from a CAD model. Case 2: We add  $N(0, 0.3)$  random Gaussian noise to each point sample. The mean distance between two nearest points is about 0.3. Case 3: We add 500 random outliers that are uniformly distributed in the space. Case 4: We remove a part of points from the point cloud. All cases are shown in the first row of Figure 4.

As shown in Figure 4, to some extent, all three methods are robust to noise, outliers, and missing parts. More specifically, Poisson surface can produce the smoothest

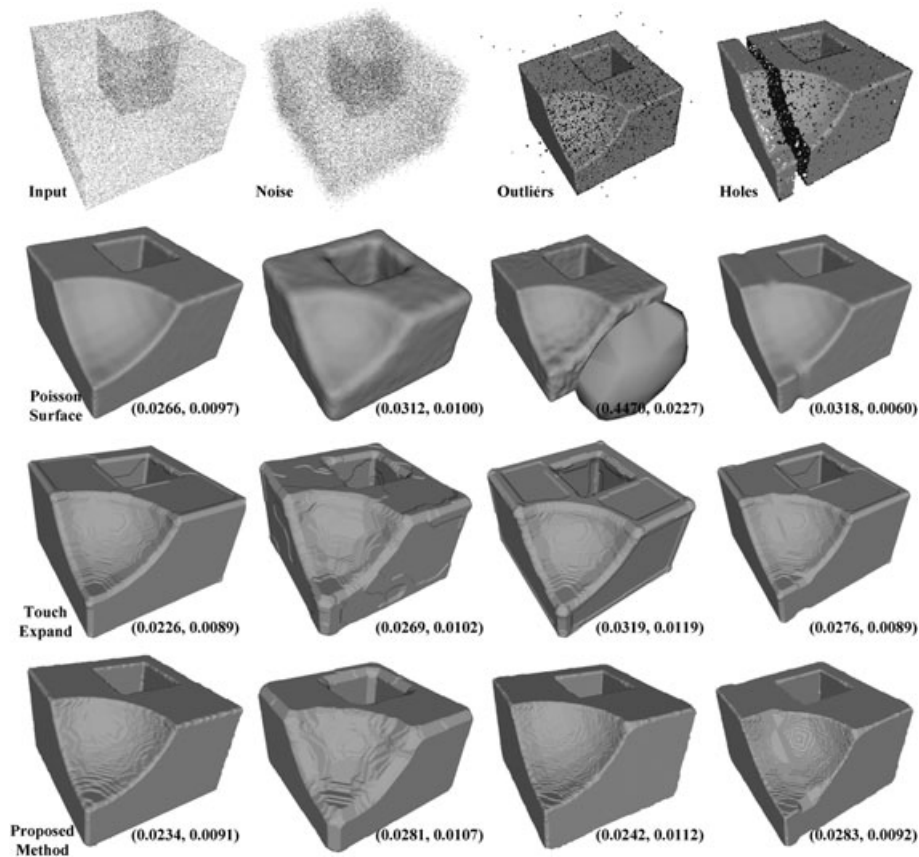


**Figure 4.** Comparison of our method with Poisson surface and touch expand on the CAD dataset. The quantitative results in terms of Hausdorff distance (first number) and root mean square error (second number) are given. The proposed method is robust to all cases and preserves sharp edges.

reconstructed surface among the three methods but is most sensitive to the outliers. Touch expand is robust to all cases; however, the surface patches around sharp features are overfitted. By contrast, our method does not suffer from these issues, and the reconstruction errors are very close to the smallest values among all results.

## 6.2. Fitting to Multiview Stereo Data

We also tested our method on MVS data, which contain more noise, outliers, and missing parts owing to the wrong photoconsistent matching errors, as shown in Figures 5(b) and 6(a).

For indoor MVS data, Poisson surface reconstructs the smoothest surface. However, it loses most detail features in Temple dataset, shown in Figure 5(c). To recover these features, we decrease the Gaussian filter radius in touch expand method, but it becomes sensitive to the noise and outliers, as illustrated in Figure 5(d). Comparing the three methods, our method reconstructs a comparable result with Poisson surface but keeps more details (Figure 5(e)). From the quantitative evaluation results, we can see that all three methods achieve nearly the same accuracy and significantly improve the reconstruction completeness. It also means that the RWLS filter can preserve detail features in appearance without loss of accuracy (Reconstruction accuracy mainly depends on the multiview stereo algorithm). Because we directly reconstruct surface from noisy points

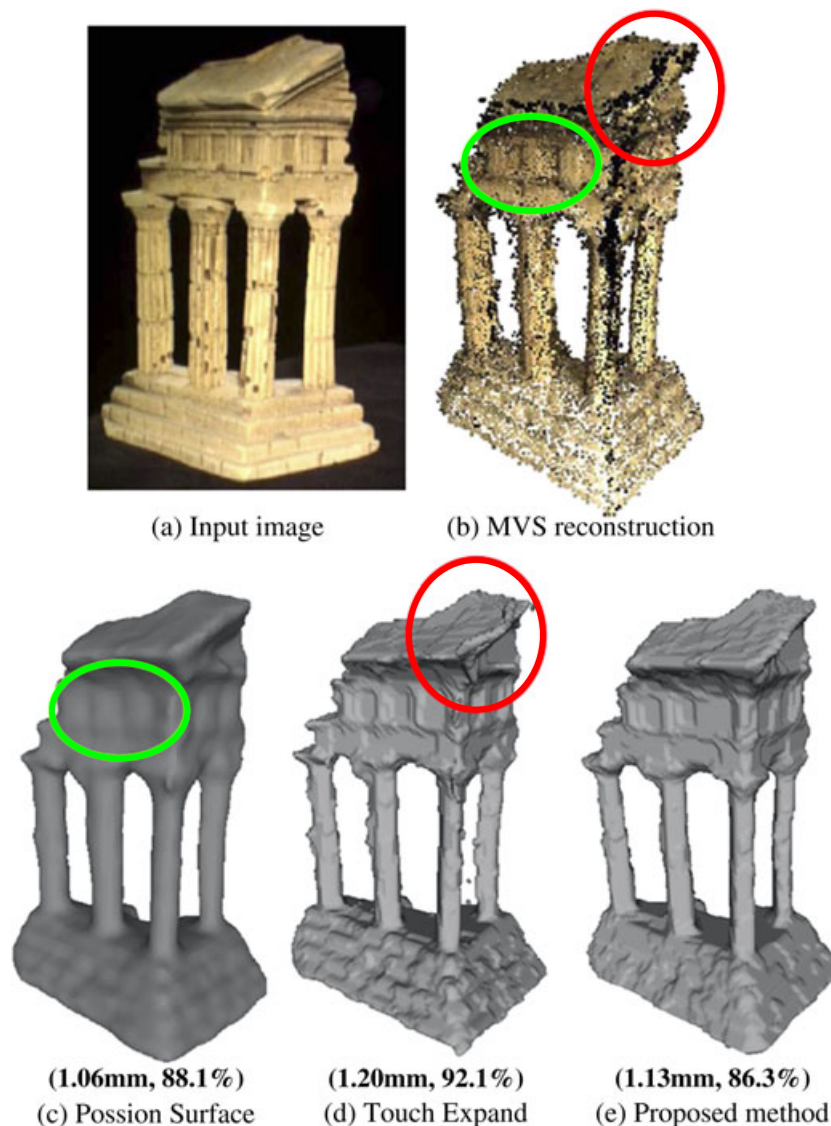


**Figure 5.** Comparison of our method with Poisson surface and touch expand on indoor MVS dataset. The proposed method can recover most details and is insensitive to the wrong matching points.

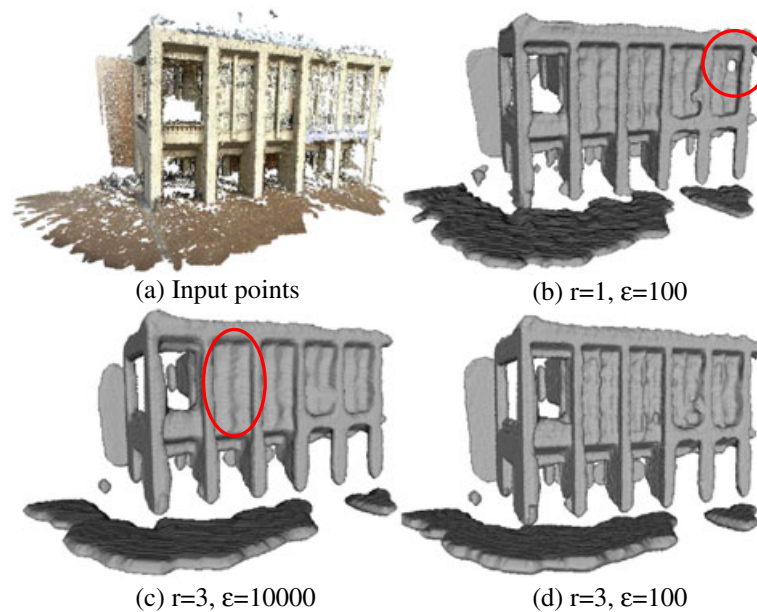


**Figure 6.** Surface reconstruction on the outdoor MVS dataset (hall) with different parameters. The regularized weighted least squares filter radius mainly affects the scene structures, whereas the regularization parameter can easily control the detail levels.

and do not refine it on the basis of photometric consistency, some results are not as good as the submitted models in the Middlebury website [2].

For outdoor MVS data, point cloud is usually incomplete and contains more noise and outliers that Poisson surface cannot work with. By contrast, our method can easily make the tradeoff between reconstruction completeness and detail feature preservation, as shown in Figure 6(d). Moreover, we analyze how the RWLS filter parameters affect the surface reconstruction result. If we set a small filter radius, detail features are preserved, but some holes appear owing to the low sampling rates in these parts (Figure 6(b)). When we increase the regularization parameter, the reconstructed surface will become smooth but will lose detail features (Figure 6(c)). For applications, users can manually adjust parameters to meet their requirements.

## 7. CONCLUSION

In this paper, we have presented a novel surface reconstruction method that can completely recover scene structures and preserve surface wrinkles or sharp features from noisy point samples. This is mainly due to the nice property of 3D RWLS filter, which balances between reconstructing a smooth surface and reproducing details. Our method also provides a basic framework to apply other filters (e.g., anisotropic filter and bilateral filter) to process noisy 3D point clouds. Moreover, our method is robust to noise,

outliers, and missing parts, and it is more suitable for passive 3D acquiring systems such as indoor/outdoor multi-view stereo system.

The main limitation of our method is that the surface reconstruction results are seriously dependent on the chosen parameters, including volume resolution, filter radius, and regularization parameter. Although we have presented a method to determine these parameters for most cases, further adjustment is sometimes needed to achieve the best appearances. In some cases, when the surface of the reconstructed object is inherently smooth, the Poisson surface yields a more reasonable result than ours because of the discretization errors introduced in the discrete graph cut phrase. Besides, features smaller than a grid cell cannot be well reconstructed. It seems that increasing the volume resolution may improve the reconstruction results. However, in practice, the effect is limited by the (uncertain) point's density. In the future, we will consider improving our method without turning any parameters and applying continuous graph cut to avoid the discretization errors.

## ACKNOWLEDGEMENTS

This work is supported by the National 863 Program of China under grant no. 2012AA011803, the Natural Science Foundation of China under grant no. 61170188, the National 973 Program of China under grant no. 2009CB320805, and the Fundamental Research Funds for the Central Universities of China.



## REFERENCES

1. Gross M, Pfister H. *Point-Based Graphics*. Morgan Kaufman, San Francisco, CA, USA, 2007.
2. Seitz SM, Curless B, Diebel J, Scharstein D, Szeliski R. A comparison and evaluation of multi-view stereo reconstruction algorithms, In *Proceedings of Computer Vision and Pattern Recognition*, Washington, DC, USA, 2006; 519–528.
3. Strecha C, von Hansen W, Van Gool L, Fua P, Thoennessen U. On benchmarking camera calibration and multi-view stereo for high resolution imagery, In *Proceedings of Computer Vision and Pattern Recognition*, Anchorage, AK, 2008; 1–8.
4. Kazhdan M, Bolitho M, Hoppe H. Poisson surface reconstruction, In *Proceedings of Symposium on Geometry Processing*, Cagliari, Sardinia, Italy, 2006; 61–70.
5. Lempitsky V, Boykov Y. Global optimization for shape fitting, In *Proceedings of Computer Vision and Pattern Recognition*, Minneapolis, 2007; 1–8.
6. Curless B, Levoy M. A volumetric method for building complex models from range images, In *Proceedings of SIGGRAPH'96*, New York, USA, 1996; 303–312.
7. Carr JC, Beatson RK, Cherrie JB, Mitchell TJ, Fright WR, McCallum BC, Evans TR. Reconstruction and representation of 3D objects with radial basis functions, In *Proceedings of SIGGRAPH'01*, New York, USA, 2001; 67–76.
8. Alexa M, Behr J, Cohen-Or D, Fleishman S, Levin D, Silva CT. Computing and rendering point set surfaces. *IEEE Transactions on Visualization and Computer Graphics* 2003; **9**(1): 3–15.
9. Guennebaud G, Gross M. Algebraic point set surfaces, In *Proceedings of SIGGRAPH'07*, San Diego, California, 2007; 23–33.
10. Oztireli C, Guennebaud G, Gross M. Feature preserving point set surfaces based on non-linear kernel regression. *Computer Graphics Forum* 2009; **28**(2): 493–501.
11. Farbman Z, Fattal R, Lischinski D, Szeliski R. Edge-preserving decompositions for multi-scale tone and detail manipulation. *ACM Transactions on Graphics* 2008; **27**(3): 1–10.
12. He K, Sun J, Tang X. Guided image filtering, In *Proceedings of the European Conference on Computer Vision*, Berlin, Heidelberg, 2010; 1–14.
13. Boissonnat J-D. Geometric structures for three-dimensional shape representation. *ACM Transactions on Graphics* 1984; **3**: 266–286.
14. Edelsbrunner H, Mücke EP. Three-dimensional alpha shapes. *ACM Transactions on Graphics* 1994; **13**: 43–72.
15. Amenta N, Bern M, Kamvysselis M. A new Voronoi-based surface reconstruction algorithm, In *Proceedings of SIGGRAPH'98*, New York, USA, 1998; 415–421.
16. Kolluri R, Shewchuk JR, O'Brien JF. Spectral surface reconstruction from noisy point clouds, In *Proceedings of symposium on geometry processing*, New York, USA, 2004; 11–21.
17. Alliez P, Cohen-Steiner D, Tong Y, Desbrun M. Voronoi-based variational reconstruction of unoriented point sets, In *Proceedings of Symposium on Geometry Processing*, Barcelona, Spain, 2007; 39–48.
18. Labatut P, Pons J-P, Keriven R. Robust and efficient surface reconstruction from range data. *Computer Graphics Forum* 2009; **28**(8): 2275–2290.
19. Salman N, Yvinec M, Merigot Q. Feature preserving mesh generation from 3D point clouds. *Computer Graphics Forum* 2010; **29**(5): 1623–1632.
20. Hornung A, Kobbelt L. Robust reconstruction of watertight 3D models from non-uniformly sampled point clouds without normal information, In *Proceedings of Symposium on Geometry Processing*, Cagliari, Sardinia, Italy, 2006; 41–50.
21. Boykov Y, Kolmogorov V. Computing geodesics and minimal surfaces via graph cuts, In *Proceedings of the International Conference on Computer Vision*, Nice, France, 2003; 26–33.
22. Chauve A-L, Labatut P, Pons J-P. Robust piecewise-planar 3D reconstruction and completion from large-scale unstructured point data, In *Proceedings of Computer Vision and Pattern Recognition*, San Francisco, USA, 2010; 1261–1268.
23. Lafarge F, Keriven R, Bredif M, Vu H-H. Hybrid multi-view reconstruction by jump-diffusion, In *Proceedings of Computer Vision and Pattern Recognition*, San Francisco, USA, 2010; 350–357.
24. Lempitsky V. Surface extraction from binary volumes with higher-order smoothness, In *Proceedings of Computer Vision and Pattern Recognition*, San Francisco, USA, 2010; 1197–1204.
25. Crow FC. Summed-area tables for texture mapping. *ACM Transactions on Graphics* 1984; **18**: 207–212.
26. Furukawa Y, Ponce J. Accurate, dense, and robust multi-view stereopsis. *IEEE Transactions on Pattern Analysis and Machine Intelligence* 2010; **32**(8): 1362–1376.

## AUTHORS' BIOGRAPHIES



**Xu Zhao** is a PhD student in the State

Key Lab of Virtual Reality Technology and Systems at Beihang University. He received the BS degree in Computer Science (2006) from Beihang University. His research interests include computer graphics, computer vision, and digital geometry processing. He is a student member of the CCF, ACM, and IEEE.



**Zhong Zhou** is an associate professor at the State Key Lab of Virtual Reality Technology and Systems, Beihang University, Beijing, China. He received his BS degree from Nanjing University and PhD degree from Beihang University in 1999 and 2005, respectively. His main research interests include tele-immersion, natural phenomena simulation, distributed virtual environment, and Internet-based VR technologies. He is a member of the CCF, ACM, and IEEE.



**Ye Duan** is an Associate Professor of Computer Science at the University of Missouri-Columbia. He received his BA degree in Mathematics from Peking University in 1991. He received his MS degree in Mathematics from Utah State University in 1996. He received his MS and PhD degree in Computer Science from the State University of New York at Stony Brook in 1998 and 2003. His research interests include computer graphics and visualization, biomedical imaging and computer vision, geometric and physics-based modeling, virtual reality and human-computer interaction, and computer animation and simulation.



**Wei Wu** is a professor in the School of Computer Science and Engineering at Beihang University, currently the chair of the Technical Committee on Virtual Reality and Visualization (TCVRV) of the China Computer Federation (CCF). He received the PhD degree from Harbin Institute of Technology, China, in 1995. He has published more than 90 papers, 33 issued patents, and one book. His current research interests involve real-time 3D reconstruction, remote immersive system, and augmented reality.